

NANOFLOWER-LIKE ZnO FILMS PREPARED BY MODIFIED CHEMICAL BATH DEPOSITION: SYNTHESIS, OPTICAL PROPERTIES AND NO₂ GAS SENSING MECHANISM

F. ÖZÜTOK^{a*}, S. DEMİRİ^b

^aPhysics Department, Çanakkale Onsekiz Mart University, 17020, Çanakkale, Turkey

^bMaterials Science and Engineering, Çanakkale Onsekiz Mart University, 17020, Çanakkale, Turkey

In the present work, nanoflower-shape zinc oxide (ZnO) films synthesized by modified chemical bath deposition (CBD). The optimum working temperature and pH was determined 50±5 °C and 9.8, respectively. Conditioning solution can functioned as an adhesive in CBD process which have been used for the first time. The effect of annealing temperature (450, 500 and 550 °C) was studied and the changing structural, elemental and morphological properties were investigated by using XRD, EDX and SEM devices, respectively. All polycrystalline films had [002] preferential orientation and the maximum crystallization was observed in ZnO films that annealed at 500 °C. Detailed optical properties (absorption, band gap energy) were investigated by using Uv-Vis spectroscopy. Optical transmittance spectra showed high optical absorption below to 370 nm in the range 300-900 nm. Gas sensing mechanism for 0.5 ppm NO₂ gas was investigated by using home-made gas sensing chamber that sensor working at 200 °C and nano-flower dimensions severely affected to gas sensitivities.

(Received March 1, 2017; Accepted April 18, 2017)

Keywords: ZnO films, characterization, annealing temperature, chemical bath deposition, NO₂ gas sensing

1. Introduction

Recently, high quality metal oxide semiconductor production has been so important due to increasing need of inexpensive, selective and sensitive gas sensing devices. Because metal oxides (i.e. SnO₂, ZnO, Fe₂O₃ and etc.) have superior properties such as low cost, simple usage, high selectivity/sensitivity at ppb/ppm levels and large surface area for detecting target gas but gas sensing mechanism is still complicated. Among them stoichiometric ZnO is a II-VI group material which has specific and tuning properties such as large band gap energy (3.37 eV), high exciton binding energy (60 meV), highly porous surfaces for reacted to gas molecules and large surface/volume ratio.

Chemical bath deposition (CBD) is so preferred film synthesis technique compared to others (i.e. spin coating, atomic layer deposition, spray pyrolysis and etc.) because of attractive properties such as applicable to large surfaces, easy set-up, working at low temperatures (<100 °C) and non-vacuum ambient [1-2]. Adherent and homogeneous film synthesis is a basic problem for this method because of un-control on the film growth depending on unforeseeable chemical reactions. Therefore complex agent using in alkaline solution has been preferred in many similar studies [3-4]. Complex agents are generally chosen as diethanolamine (DEA), triethanolamine (TEA), monoethylamine (MEA), ethylenediamine (EDA), ammonia, dimethylamine (DMA) and their mixtures [5-6].

Many studies drew the attention the complex agent effect on ZnO film growth. Taofeek et. al observed that ions-by-ions deposition for EDTA and clusters-by-clusters deposition for DMA [7]. Another study received by Taunk et al. that band gap increases with decreasing the concentration of TEA [8]. A study received by Inamdar et.al. that granular and compact structures were obtained with

*Corresponding author: fatmaozutok@comu.edu.tr

using EDTA and citric acid respectively [9]. Despite of these studies, adherent and homogeneous film obtaining is still a big issue in CBD.

In this paper, modified CBD was used for obtaining ZnO films onto glass substrate and the effect of annealing temperature was investigated on the structural, elemental and morphological properties of ZnO films. Modified CBD includes a conditioning solution which occurs diluted TEA/ammonia mixing for this study. It acts as a adhesive between the corning glass and deposited layer. Also, optical (absorption, transmittance and direct band gap) and NO₂ gas sensing properties were studied.

2. Experimental

2.1. Preparation of ZnO Films

All chemicals obtained from Sigma–Aldrich without further purification. Firstly, corning glasses were used as a substrate, cutted to 80*80 mm and standart glass cleaning procedure (dipped in ethanol, acetone and distilled water and dried in air during a one day, respectively) was applied [10]. Conditioning solution occurs mixture of TEA/ammonia/distilled water that volume ratios are 2:4:25. The glasses were left in the conditioning solution for 15 minutes before dipping. Then, glasses dipped into the Zn-ammonia based solution (Zn/NH₃: 1/10) and Zn-source was zinc acetate dihydrate (pH=9.8). The optimum working temperature and dipping time was determined by 50±5 °C and 5 minutes, respectively. Only the use of Zn-ammonia based solution caused the precipitation and time extension (>10 minutes) under similar deposition process and film quality severely decreased as shown Fig.1(a). All of the films dried at 100 °C after deposited on the substrate. Finally, ZnO films annealed at 450, 500 and 550 °C temperature for 1 hour in the furnace.

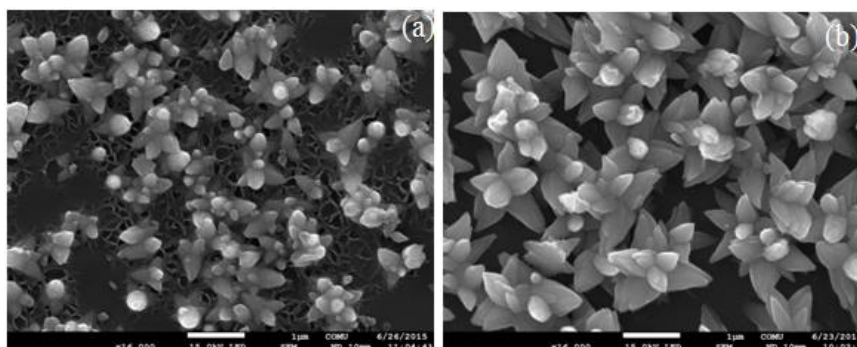


Fig.1. SEM images of ZnO thin film a) CBD b) CBD with conditioning solution under similar process

2.2. Characterization of ZnO Films

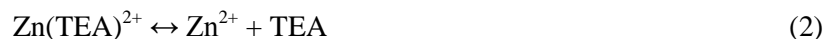
The structural composition of the ZnO films was characterized by Rigaku SmartLab XRay Diffractometre with CuK_α (1.5406 Å) which was operated at 40 KV and 30 mA. The structural morphologies of the samples were carried out by JEOL JSM-7100 F-SEM device which was worked at 8x10⁻¹ mbar/Pa vacuum operator, 10 mA current and Au-Pd (80-20 %) coating. Elemental analysis was dedected by OXFORD Instruments X-Max-EDX device. SEM and EDX devices connected to each other. Optical properties were investigated by Analytic Jena Uv-Vis spectroscopy that obtained in 300-900 nm. wavelength range. Direct band gap energies depending on the film thickness and grain sizes calculated by Debye-Scherer formula and Tauc model, respectively. Home-made gas-sensing chamber was used to detection of 0.5 ppm NO₂ gas that was repeated 3 times.

2.3. Film Growth

CBD consists of two stages which one is nucleation another is particle growth. Details of the stages for nano-flower shape ZnO structures have been given by Ahsanulhaq et.al. and Wang et.al.

[11-12]. Unlike other studies, before the nucleation stage substrate coated aqueous mixing complex agents (TEA and ammonia) in this work so decompose of complex agents was smoothed. Mixing complex agents easily interacted with $[\text{Zn}(\text{OH})_4]^{2-}$ and $\text{Zn}(\text{OH})_2$ clusters on the substrate and heterogeneous reactions formed rapidly into the solution. Then, the density of the clusters were decreased at working temperature so the homogeneous ZnO film was obtained. Also, annealing effect can provide remove to accumulate molecule groups on the surface.

Possible chemical reactions of film growth by the following equations;



3. Results and Discussion

3.1. Structural Properties of ZnO Films

The XRD patterns of pristine and annealing ZnO films were shown in Fig.2 and all of the samples are observed polycrystalline form. The all of the diffraction peaks corresponding to hexagonal wurtzite crystal structure and the cell constants can match the standard JCPDS: 36-1451 card. There are no characteristic impurities peaks, i.e. Zn or $\text{Zn}(\text{OH})_2$ that detected within detection limits of XRD technique. A broad diffusion peak centered between $2\theta=20^\circ$ and $2\theta=30^\circ$ range which is originated from amorphous glass. It was observed that especially in the pristine ZnO samples and it could be reduced by the annealing effect.

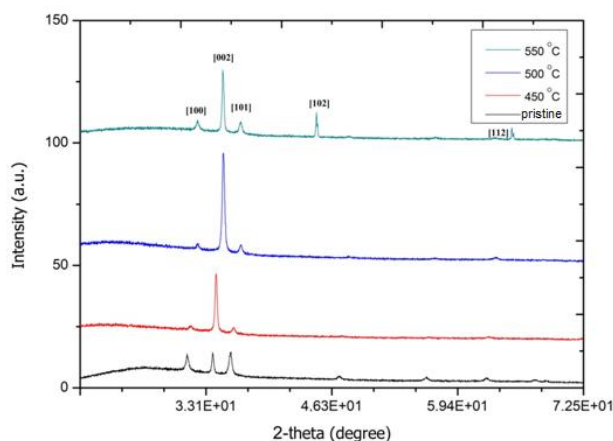


Fig. 2. XRD patterns of ZnO thin films under different annealing temperatures

Three evident different diffraction (2θ) peaks are 31.74° , 34.40° and 36.20° corresponding to [100], [002] and [101] planes, respectively. Strong [002] preferential peak is shown on c -axis orientation so grains are mainly grown with c -axis vertical to the substrate and intensity of this peak also alters with the annealing effect [13]. Also, low intensity [100] and [101] peaks are showed and

they are affected orientation slightly. The best crystallization level and therefore minimum surface defects were observed in ZnO samples that annealed at 500 °C. It was observed that the shifts in peak positions related to deformation in the crystal lattice due to the increase of the oscillation energy of atoms and thus may occurred rearrangement of surface atoms [14]. Also, changing FWHM values and intensities of [100] and [101] peaks originated from defects and strain effect and it was clearly explained by Dutta et.al. [15].

As shown in Fig.3., increasing of annealing temperature up to 500 °C caused grain size decreasing. But, with increasing of annealing temperature from 500 °C to 550 °C caused grain size increasing. This indicates that at temperatures above 500 °C the stress has increased along the interfaces depending on the changing native imperfections.

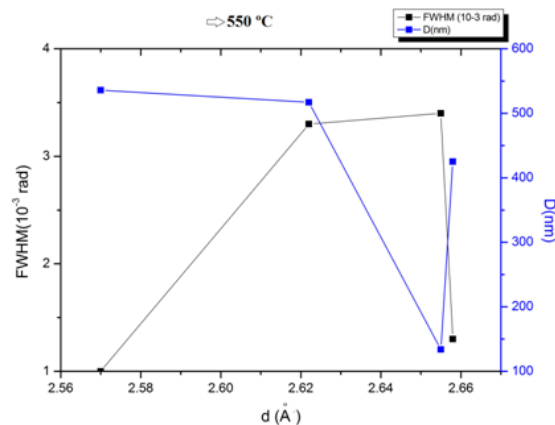


Fig.3. Variation of structural properties [d (interplanar distance), $FWHM$ (half peak width) and D (grain size)] for ZnO films under different annealing temperatures

3.2. Surface Morphology of ZnO Films

All of the SEM images were taken at magnification ratio of 16000 in the selected area. As given by Fig. 4., ZnO films have nano-flower and nano-petal formations that have been disturbed relatively homogeneous on the corning glass surface. Dimensions of nano-flower formations can change with the annealing temperature, severely. Average dimensions of nano-petal formations are changed by between in 150-300 nm. range. Increasing of annealing temperature up to 500 °C caused a decrease on the density of flower-shape forms and then increasing up to 550 °C caused an increase on the density of flower-shape forms and this finding correlated to results in Fig.3. In addition to, crystal planes aligned perpendicularly to the c-axis growth direction that was explained by XRD patterns. Also, as shown in Fig.5. the nucleus part contains 16 % more zinc element than the leaf part which is confirmed by EDX analysis results.

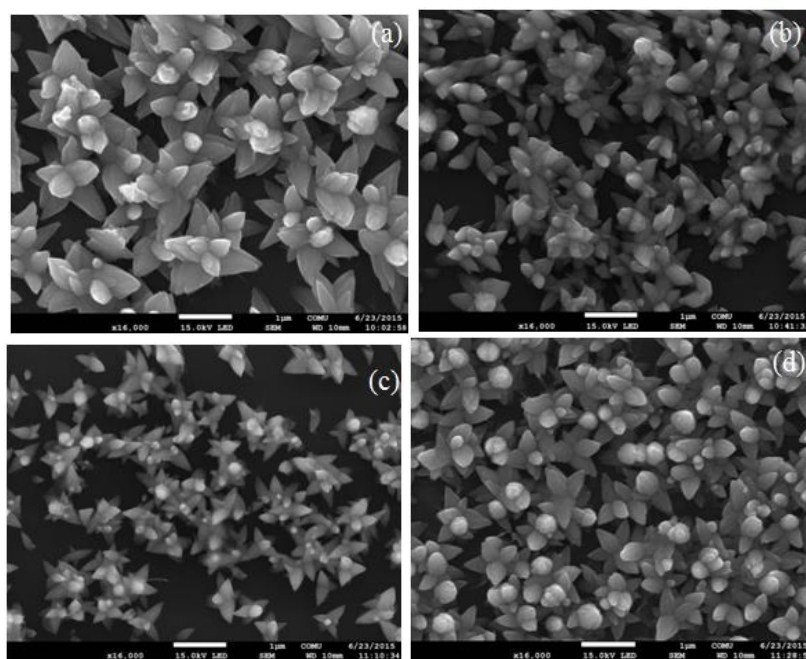


Fig. 4. SEM images of ZnO thin films under different annealing temperatures a) pristine b) 450 °C c) 500 °C and d) 550 °C, respectively

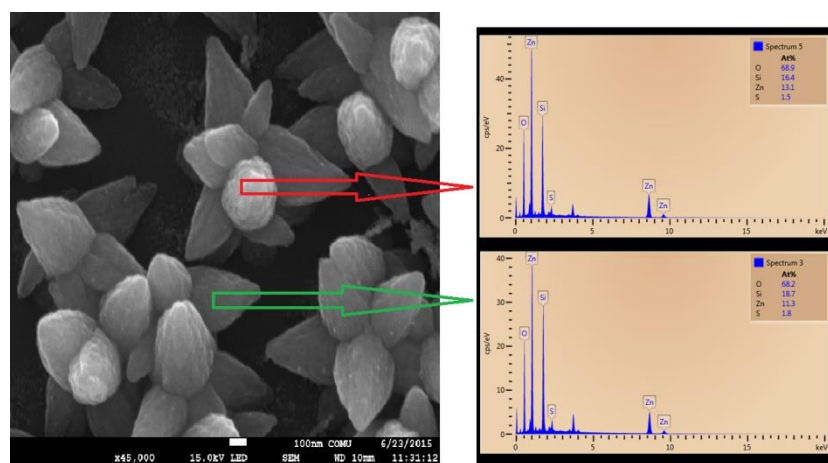


Fig.5. Detailed SEM image of nano-flower ZnO film

3.3. Elemental Analysis Results of ZnO Films

Elemental compositions of all the films were received in Fig.6. Silisium and calcium peaks originated from glass substrate. Expected both elements (zinc and oxygen) were observed and impurity elements were not found. High oxygen ratio (> 50 %) arised from OH^- ions in alkaline solution which was explained by Allouche et.al.[16]. The annealing temperature severly affected the ratio of the elements especially oxygen ratio. Because OH^- ve O^{2-} - based ion groups be able to removed from the surface by the annealing effect.

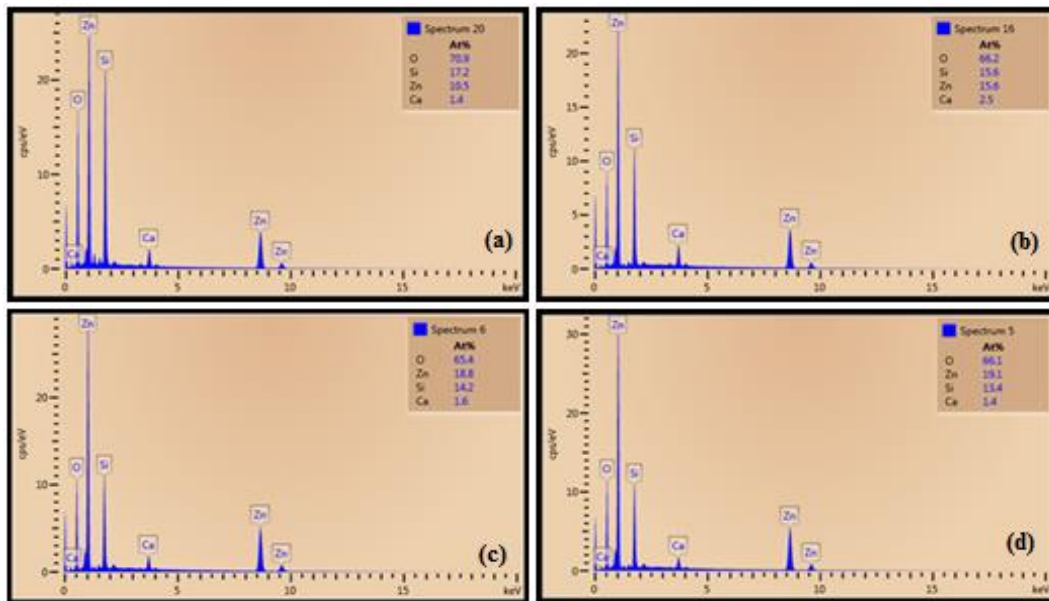


Fig. 6. EDX analysis results of ZnO films under different annealing temperatures a) pristine b) 450 °C c) 500 °C and d) 550 °C, respectively

3.4. Optical Properties of ZnO Films

Optical absorption spectrum of all ZnO thin films were given in Fig. 7. The decrease in the optical absorption of ZnO films was related to decrease nano-flower dimensions. It indicates that crystallization (from XRD patterns) and dimension of nano-flowers (from SEM images) can affect optical behaviour of the films. Optical absorption tail is coordinated at 370 nm. and observed fluctuations are related to oxygen-based impurities [17].

Calculation of the absorption coefficient (α) depending on the film thickness (d) and also band gap energy (E_g) depending on direct transition according to Tauc plots model were given many studies in the literature but it was ignored experimental limitations [18]. The optical band gap determined as given relationship;

$$(\alpha h\nu)^2 = A (h\nu - E_g)^n \quad (n=1/2 \text{ for direct allowed transitions}) \quad (7)$$

where; $h\nu$ is the photon energy, E_g is the optical band gap energy and A is a constant. The determination of direct band gap is calculated by extrapolating the linear portion of $(\alpha h\nu)^2$ to $h\nu = 0$ point.

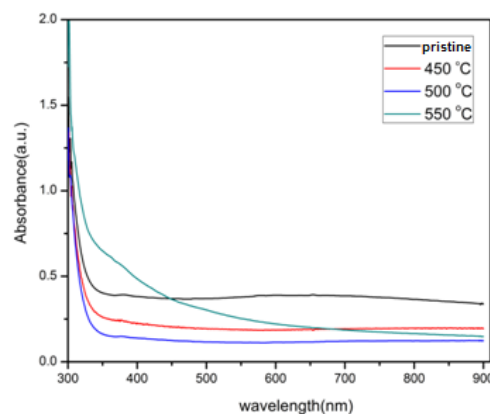


Fig. 7. Optical absorption spectra of pristine and annealed ZnO films

Tauc model's evaluation and fitting was studied by Viezbicke et.al. [19]. Fig.8. shows the fitted direct band gap energy values of ZnO samples and changed between in 2.78 eV-3.21 eV range and these values compatible to literature with using CBD [20]. Enhancement on the direct band gap (called as blueshifted) energies may occurred by two probable way; one is improved crystallization and decreased surface defects especially which arising with oxygen-based impurities and another is transformation from Zn(OH)₂ to pure ZnO [21].

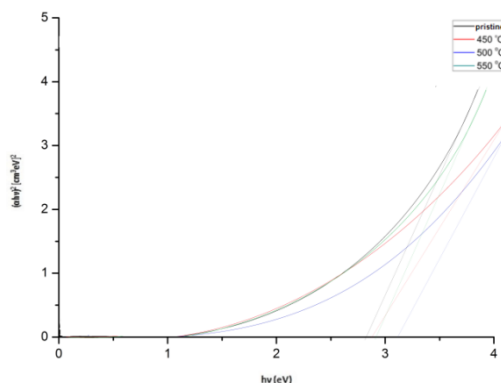


Fig. 8. Direct band gap energy (E_g) of ZnO films under different annealing temperature

3.5. NO₂ Gas Sensing Mechanism of ZnO films

Sensing measurements of ZnO films against to 0.5 ppm periodic exposure of NO₂ gas were showed in Fig.9., measuring at 200 °C. Below the sensor working temperature of 200 °C it wasn't detected any signal because of the statical recovery kinetics. NO₂ has oxidizing gas character and adsorbed oxygen species (i.e. O₂⁻, O²⁻ and O⁻) have an important role in gas sensing mechanism and this difference depends on the sensor temperature severly [22]. Also, oxygen-based impurities act as adsorption sites that gives an enormous contribution for gas testing and this effect was investigated by Nisha et.al. [23]. Exposing NO₂ gas molecules to ZnO grains adsorbed oxygen species (O⁻ character for sensor temperature of 200 °C) are reacted with them on the surface according to this equation;



ZnO is n-type material naturally and oxidizing gas induces a depletion in sensing layer therefore occurs a decrease in conductivity that was explained by Fine et.al. and similar situation showed in Fig.9 [24].

In Fig. 9(a), gas sensing behaviour of pristine samples different than other samples because most of the OH⁻ ions could not be removed from the film surface and NO₂ gas adsorption got worsen. Introducing electrons showed directly behaviour that caused an increase the conductivity. Therefore the annealing of films has improving effect on the NO₂ gas sensitivity mechanism so grain sizes have been decreased and porous gas sensitivity surface area have been increased. It was detected that ZnO films that annealed at 500 °C had maximum sensitivity compared to other samples. On the other hand, the annealing at high temperatures (>500 °C) is generated field by the surface adsorbed oxygen ions so causes exposed chemical bonds yielding. Therefore all of the chemical bonds on the surface may reacted with oxygen molecules and there is no open bonds. It is therefore important to reduce the gas sensing properties on an optimal annealing temperature. Also, the annealing at high temperatures (>500 °C) can lead to deterioration on the substrate/deposited layer interface.

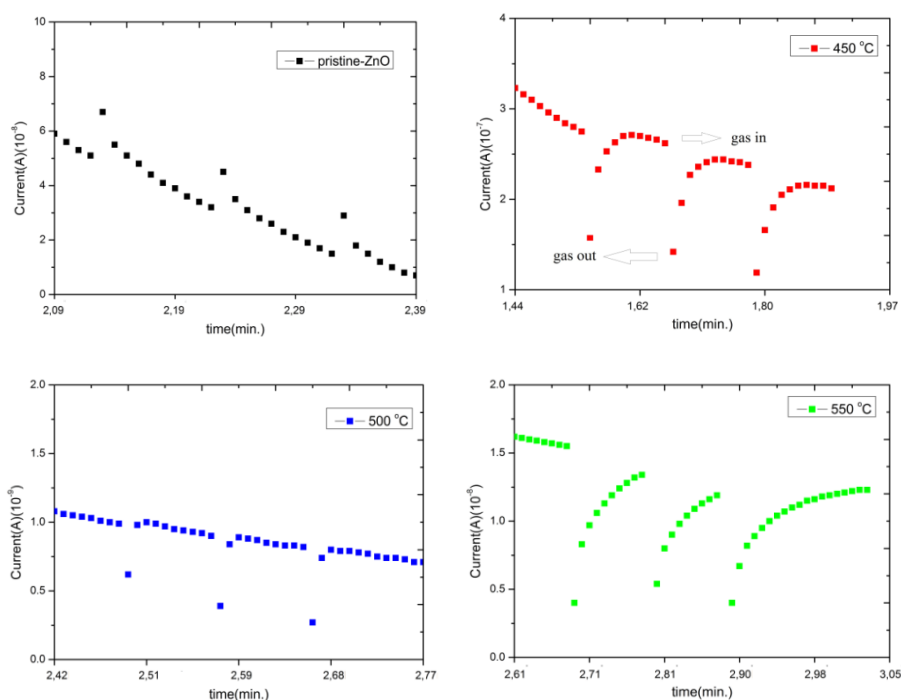


Fig. 9. 0.5 ppm NO_2 gas sensitivity of ZnO films which were measured at 200 °C

4. Conclusions

In the present work, ZnO films were prepared by modified chemical bath deposition under different annealing temperatures. It could be obtained adherent and homogeneous films with using of conditioning solution which not being in the literature. All of the films have hexagonal wurtzite crystal structure and [002] preferential orientation which confirmed by x-ray diffractometer. Also, all films have flower-like shape structure and their dimensions have changed depending on the annealing temperature. This study suggests a correlation between the flower dimension and optical (also NO_2 gas sensing) behaviour of the synthesized materials. It is thought that different type conditioning solutions can be prepared for II-V materials in the subsequent studies.

Acknowledgments

This work was supported by the Council of Scientific Research Project (Grant number: FDK-2015-470).

References

- [1] A. Jilani, J. Iqbala, S. Rafiquea, M.S. Abdel-wahaba, Y.Jamil, A. A. Al-Ghamdi, *Optik* **127**, 6358 (2016).
- [2] Nagarani Nagayasamy, Saroja Gandhimathination, Vasu Veerasamy, *Open Journal of Metal* **3**, 8 (2013).
- [3] Z. R. Tian, J. A. Voigt, J. Liu, B. Mckenzie, M. J. Mcdermott, M. A. Rodriguez, H. Konishi, H. Xu, *Nature Materials* 2003, 821.
- [4] L. Chen, D. Zhang, Q. Chen, *Proceedings of the 1st IEEE International Conference on Nano/Micro Engineered and Molecular Systems* 2006, <https://doi.org/10.1109/NEMS.2006.334853>.

- [5] H. Khallaf, G. Chai, O. Lupan, H. Heinrich, S. Park, A. Schulte, Lee Chow, *J. Phys. D: Appl. Phys.* **42**, 135304 (2009).
- [6] A.K. Singh, S.B. Patil, V. C. Janu, *IEEE xplore* 2008, 978-860.
- [7] Y. G. Taofeek, E.H. Olusegun, *International Journal Of Scientific & Technology Research* **1**, 8 (2012).
- [8] P. B. Taunk, R. Das, D. P. Bisen, R.K. Tamrakar, Nootan Rathor, *Karbala International Journal of Modern Science* **1**, 159 (2015).
- [9] A. I. Inamdar, S. H. Mujawar, P. S. Patil, *Int. J. Electrochem. Sci* **2**, 797 (2007).
- [10] M.S. Sameem, *IJRSET* **2**, 1 (2015).
- [11] Y. Wang, X. Li, N. Wang, X. Quan, Y. Chen, *Separation and Purification Technology* **62**, 727 (2008).
- [12] Q. Ahsanulhaq, S.H. Kim, J.H. Kim, Y.B. Hahn, *Materials Research Bulletin* **43**, 3483 (2008).
- [13] M. Shaban, M Zayed, H. Hamdy, *RSC.Adv.* **7**, 617 (2017).
- [13] Z. Lin, L.V. Zhigilei, *Journal of Physics: Conference Series* **59**, 11 (2007).
- [14] S. Dutta, S. Chattopadhyay, A. Sarkar, M. Chakrabarti, D. Sanyal, D. Jana, *Progress in Materials Science* **54**, 89 (2009).
- [15] N.K.Allouche, T.B. Nasr, N.T. Kamouna, C. Guasch, *Materials Chemistry and Physics* **123**, 620 (2010).
- [16] M. Willander, O. Nur, J.R. Sadaf, M. I. Qadir, S. Zaman, A. Zainelabdin, N. Bano, I.Hussain, *Materials* **3**, 2643 (2010).
- [17] Gurpreet Kaurn, Anirban Mitra, K.L. Yadav, *Progress in Natural Science: Materials International* **25**, 12 (2015).
- [18] B. D. Vierzicke, S. Patel, B. E. Davis, D. P. Birnie, *Phys. Status Solidi B* **252**, 8 (2015).
- [19] A. S. Dive, D. S. Upadhye, N. P. Huse, S.B. Bagul, K.P. Gattub, R. Sharma, *BIONANO FRONTIER* **8**, 3 (2015).
- [20] P.K. Baviskar, P.R. Nikam, S.S. Gargote, A. Ennaoui, B.R. Sankapal, *Journal of Alloys and Compounds* **551**, 233 (2013).
- [21] S.T. Navale, D.K. Bandgar, M.A. Chougule, V.B. Patil, *RSC.Adv.* **5**, 6518 (2015).
- [22] R.Nisha, K.N. Madhusoodanan, T.V. Vimalkumar, K. P. Vijayakumar, *Bull. Matt.Sci.* **38**, 3. (2015).
- [23] G. F. Fine, L. M. Cavanagh, A. Afonja, R. Binions, *Sensors* **10**, 5469 (2010).